Journal of Cardiovascular Computed Tomography 13 (2019) 226–233

Contents lists available at ScienceDirect

Journal of Cardiovascular Computed Tomography

journal homepage: www.elsevier.com/locate/jcct

Research paper

Evaluation of ventricular septal defects using high pitch computed tomography angiography of the chest in children with complex congenital heart defects below one year of age

David Nau[a,b,1], Wolfgang Wuest[a,c], Oliver Rompel[a], Matthias Hammon[a], Martin Gloeckler[d], Okan Toka[d], Sven Dittrich[d], André Rueffer[e], Robert Cesnjevar[e], Michael M. Lell[f], Michael Uder[a,c], Matthias S. May[a,c,*]

[a] University Hospital Erlangen, Department of Radiology, Maximiliansplatz 1, 91054, Erlangen, Germany
[b] Friedrich-Alexander-University Erlangen-Nürnberg (FAU), Schlossplatz 4, 91054, Erlangen, Germany
[c] Imaging Science Institute Erlangen, Ulmenweg 18, 91054, Erlangen, Germany
[d] University Hospital Erlangen, Department of Pediatric Cardiology, Loschgestrasse 15, 91054, Erlangen, Germany
[e] University Hospital Erlangen, Department of Pediatric Cardiac Surgery, Loschgestrasse 15, 91054, Erlangen, Germany
[f] Paracelsus Medizinische Privatuniversität Nürnberg, Prof.-Ernst-Nathan-Strasse 1, 90419, Nuremberg, Germany

ARTICLE INFO

Keywords:
Dual-source
Computed tomography angiography
Ventricular septal defect
Congenital heart defect
High pitch

ABSTRACT

Background: Aim of this study was to assess the accuracy of ventricular septal defects (VSD) using high pitch computed tomography angiography (CTA) of the chest in children below 1 year of age, compared to the intraoperative findings and echocardiography.

Methods: Out of 154 patients that underwent Dual-Source CTA of the chest using a high-pitch protocol at low tube voltages (70–80 kV), 55 underwent surgical repair of a VSD (median age 8 days, range 1–348 days). The margins of the VSDs and their relation to the surrounding structures were reproduced by en-face views using multiplanar reformations (MPR). Absolute diameter, normalized area and relative area compared to the aortic valve annulus were used for discrimination between restrictive and non-restrictive defects. Localization was classified into four subtypes. The results were compared to two-dimensional echocardiography and intraoperative findings.

Results: Median absolute size of VSDs did not differ significantly between CTA-measurements (10.8 mm, range 2.8–18.1 mm) and intraoperative findings (12.0 mm, 3.0–25.0 mm, $p = 0.09$). Echocardiographic values were significantly lower (9.6 mm, 3.0–18.5 mm, both $p < 0.01$). The classification of the location and orientation matched the intraoperative situs in 96.4% of all cases using CT and in 87.3% using echocardiography. Echocardiography missed the relation to valves in 11% of all cases. Pre-interventional sensitivity and specificity for detection of a VSD were 97.2/98.9% compared to echocardiography. Median radiation dose was 0.32 mSv (range 0.12–2.00 mSv) and differed significantly between second and third generation Dual-Source CT (0.43 vs. 0.22 mSv, $p = 0.003$).

Conclusion: Size and subtype of VSDs can be accurately assessed by CTA of the chest in patients with complex congenital heart defects at a very low radiation dose.

1. Introduction

Congenital heart disease (CHD) is a common condition with an estimated incidence of up to 10 in 1000 live births. Many of these anomalies present with ventricular septal defects (VSD) that often require surgical repair to separate the pulmonary and the systemic

* Corresponding author. University Hospital Erlangen, Department of Radiology, Maximiliansplatz 1, 91054, Erlangen, Germany.
E-mail addresses: david-nau@web.de (D. Nau), wolfgang.wuest@uk-erlangen.de (W. Wuest), oliver.rompel@uk-erlangen.de (O. Rompel), matthias.hammon@uk-erlangen.de (M. Hammon), martin.gloeckler@uk-erlangen.de (M. Gloeckler), dr.toka-mzv-fuerth@outlook.de (O. Toka), sven.dittrich@uk-erlangen.de (S. Dittrich), andre.rueffer@uk-erlangen.de (A. Rueffer), robert.cesnjevar@uk-erlangen.de (R. Cesnjevar), michael.lell@klinikum-nuernberg.de (M.M. Lell), michael.uder@uk-erlangen.de (M. Uder), matthias.may@uk-erlangen.de (M.S. May).
[1] David Nau performed the present work in partial fulfillment of the requirements for obtaining the degree “Dr. med.”

https://doi.org/10.1016/j.jcct.2019.01.023
Received 4 September 2018; Received in revised form 14 January 2019; Accepted 31 January 2019
Available online 01 February 2019

Abbreviations

CT	Computed Tomography
VSD	Ventricular septal defect
CTA	CT angiography
MPR	Multiplanar reformations
MinIP	Minimum intensity projection
CHD	Congenital heart disease
CTDIvol	Volumetric CT dose index
DLP	Dose length product
ED	Effective dose
ASD	Atrial septal defect
AVSD	Atrioventricular septal defect
MRI	Magnetic Resonance Imaging

circulation.[1] Detailed knowledge of the location, orientation and size of the VSD is essential to the pediatric cardiologist for a hemodynamic assessment and clinical workup as well as to the pediatric cardiac surgeon to select the adequate type of surgical access and the required technique of surgical repair.[2] To date two-dimensional echocardiography is routinely performed for preoperative assessment. However, three dimensional techniques are able to significantly enhance the visualization of septal defects.[3] En-face reconstructions of the VSDs have proven their benefits for the surgical procedure and the patients' outcome.[4] Cheng et al. found improved correlations for a three-dimensional echocardiography technique with the intraoperative findings. They concluded that two-dimensional echocardiography lacks the ability to display the entire shape of the septal defects and thus cannot account for precise quantification.[5] Despite these advances in echocardiography, transthoracic as well as transesophageal examinations can be limited by the individual performance of the patient and the physician, the limited reproducibility and the few angulations available.[6] Dynamic evaluation especially remains difficult in high heart rates and complex defects with close relation to the adjacent structures, such as membranous outflow tracts, valves and trabeculae. Magnetic Resonance Imaging as alternative cross-sectional modality is limited in critically ill newborn patients due to the high periprocedural effort.[7] Computed tomography (CT) was limited in the past by its radiation exposure which is highly relevant to young patients with congenital heart disease. Temporal resolution of CT has substantially increased in the recent years while the radiation dose decreased, especially for cardiovascular indications.[8] High pitch Dual-Source CT allows for examination of the entire chest within one single heart beat and therefore provides minimized motion artifacts at a very low radiation dose.[9] Especially for preoperative assessment of CHD several indications for cardiothoracic CT angiography (CTA) have been established, such as anomalies of the coronary arteries,[10] anatomy of the great intrathoracic vessels[11] and major aortopulmonary collateral arteries.[12] A multimodality approach with additional cross-sectional imaging after the initial echocardiography has been established for surgical plan in the past.[13] However, no structured data exists on the role of CTA for visualization of VSDs other than the work of Nagakawa et al., who evaluated the ventricular anatomy in general.[14] Our aim was therefore to retrospectively assess the accuracy of VSD measurements and classifications in patients with complex CHD younger than one year by high pitch cardiothoracic CT compared to the routinely performed echocardiography and the intraoperative findings.

2. Methods

2.1. Patients

Out of 2092 patients younger than one year that consulted our department of pediatric cardiology during the study period, we retrospectively evaluated the data sets of the 154 patients (7.3% of all patients) that underwent cardiothoracic CTA for preoperative workup of complex CHD between 2009 and 2015. Out of 69 patients with a VSD 55 underwent surgical repair. Patients with a VSD without surgical repair were excluded (n = 14, Fig. 1). All of the patients were routinely evaluated before surgery using 2D transthoracic echocardiography. The study complies with the Declaration of Helsinki and the Health Insurance Portability and Accountability Act and was approved by the institutional review board. The body mass index was calculated according to the formula of the world health organization and the body surface area was estimated using the Mosteller technique.[15,16]

2.2. Surgery

From the 14 excluded patients that did not undergo surgical repair of the VSD 8 underwent single ventricle palliation, 4 smaller VSDs were considered hemodynamically irrelevant and 2 patients died before a surgical intervention. Localizations of the VSDs as classified in the surgical reports served as reference. The longest diameters were used as absolute size.

2.3. Echocardiography

Transthoracic 2D echocardiography was performed using a Vivid 7 ultrasound system (GE Medical Systems, Vivid 7, Vingmed Ultrasound AS, Horten, Norway) by experienced senior cardiologists. The largest diameters in diastole from the best fitting angulation were used for this study.

2.4. CT technique

Indication to CTA was in accordance with the consensus document of the Society of Cardiovascular Computed Tomography for CHD in 53 patients.[17] Two patients were primarily examined for non-cardiac purposes (lung and esophagus) and presented an incidental VSD. None of the examinations was exclusively performed to evaluate the VSD. The examinations were performed using a second and third generation Dual-Source CT scanner (Somatom Definition Flash or Somatom Force, Siemens Healthcare GmbH, Forchheim, Germany). The institutional reference protocol for pediatric CTA of the chest as shown in Table 1 was used for all patients.

For the examination, all patients were fixed in a supine position with their arms elevated on the CT table. The scan was performed in craniocaudal direction and ranged from the upper thoracic aperture to the posterior phrenicocostal angles. Premedication was used for patients elder than 4 months (0.1 mg/kg Midazolam). Patients below the age of 4 months were examined without sedation. Contrast media (1.5–2.0 ml per kg body weight, Imeron 300, Iomeprol, Bracco Imaging,

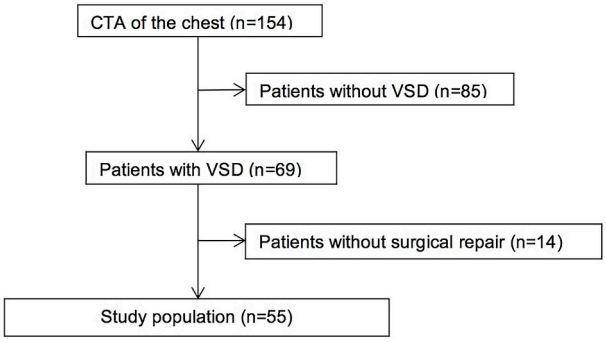

Fig. 1. Flow chart of patient selection for the study population.

Table 1
Institutional pediatric Dual Source (DS) CTA protocol for the chest. Reference tube current time product is provided as mAs per rotation following the vendors setting for cardiac protocols. The provided collimation is achieved by a z-flying focal spot.

	Second generation DS-CT	Third generation DS-CT
Tube Voltage:	80 kV	70 kV
Reference mAs:	400 ref mAs/rot	400 ref mAs/rot
Collimation	128 × 2 × 0.6 mm	192 × 2 × 0.6 mm
Pitch	3.4	3.2
Rotation Time	0.28	0.25

Konstanz, Germany) was injected manually prior to the examination with a start delay of 2 s after completion. An ECG-trace was used as trigger for automated cardiac-phase selection. Thin slices (0.6 mm) with an overlapping increment (0.3 mm) were reconstructed with matching vascular weighted filtered back projection kernels (B26f and Bv40) for image evaluation.

2.5. Image evaluation

The evaluation of the defects was performed in randomized order using a post-processing 3D console (SyngoVia, Siemens Healthcare GmbH, Erlangen, Germany). The datasets were evaluated by two senior radiologists. Multiplanar reformations (MPR) were manually adjusted to obtain two chambers, four chambers and short axis planes. The orientation of the defect was then aligned, with respect to surgical aspects

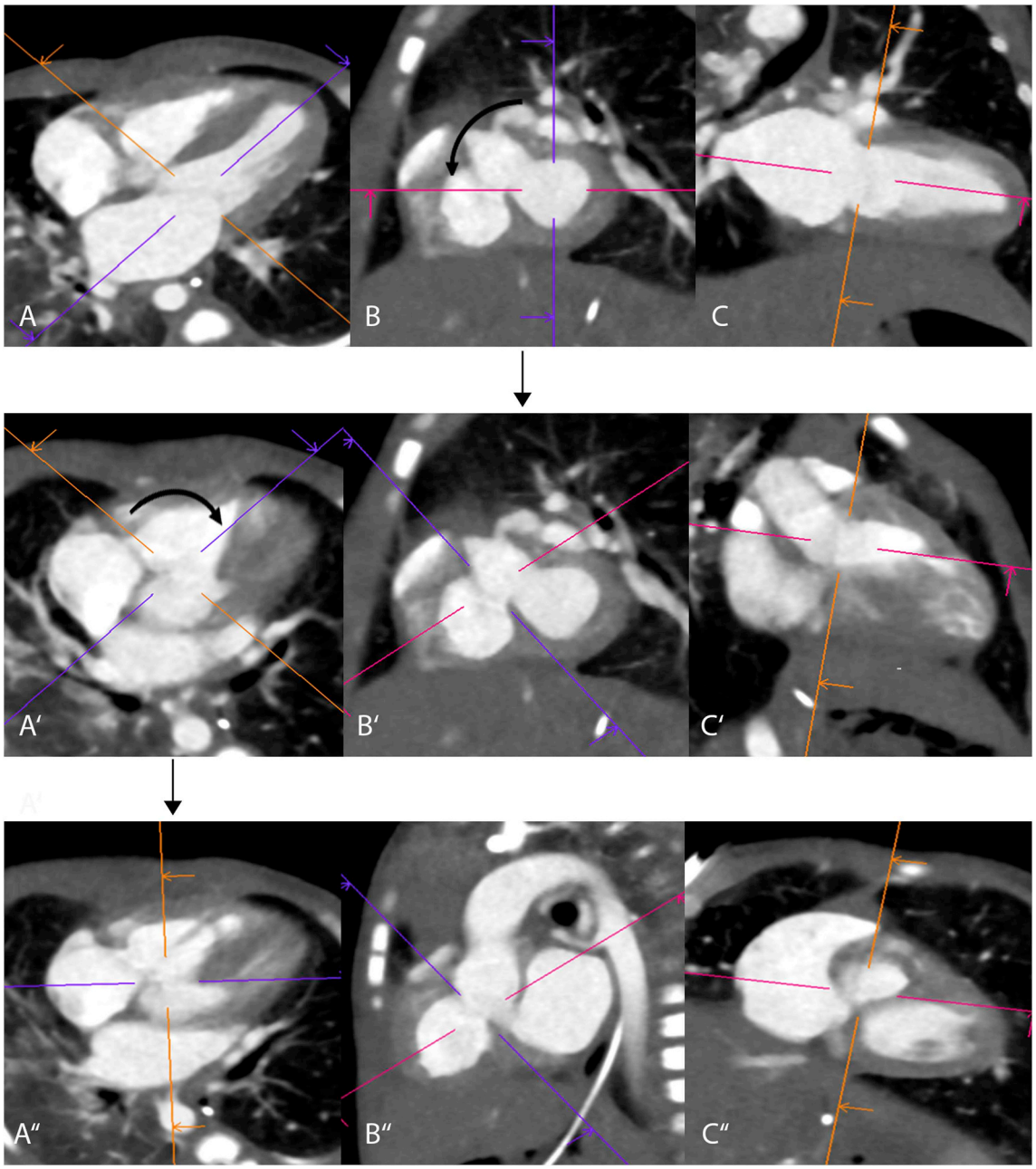

Fig. 2. Reproduction of ventricular septal defects (VSD): Seven days old boy with a tetralogy of Fallot, four chambers plane (A) and short axis plane (B) are used to obtain a preliminary en-face view on a subaortic committed VSD (Type 1) in the two chambers plane (C). Adjustments (black arrows) in the short axis plane (B to B′) and in the four chambers plane (A′ to A″) allow for sharp reproduction of the VSD (C″).

for the planned repair, in the four chambers and short axis planes to evaluate the size in the adjusted two chambers plane, simulating an en-face view (Fig. 2). To overcome partial volume effects the true lumen of the VSD was assessed by minimum intensity projection technique (MinIP) that summarizes the cardiac tissue within a contrast filled thick slice. The slice thickness was individually adjusted respecting the margins in the other planes until all edges were sharply reproduced.

2.6. Ventricular septal defects

VSD size can be classified into small, moderate and large defects using the absolute diameter (small < 10 mm, moderate 10–15 mm, large > 15 mm), the normalized area (small < 0.5 cm^2/m^2, moderate 0.5–1.0 cm^2/m^2, large > 1.0 cm^2/m^2) or the relative size referenced to the aortic annulus (small < 0.33, moderate 0.34–0.66, large > 0.66) as proposed in literature.[2] Small and moderate VSDs are considered as restrictive and large VSDs as non-restrictive. Therefore, the largest absolute diameter, its orthogonal diameter and the absolute area of the defect were manually measured. Normalized area calculation was referenced to the body surface area and relative area assessment was referenced to the area of the aortic valve annulus at the level of the valve's hinge-points. Localization of the VSD was classified into four different main types as suggested by Jacobs: Committed VSDs (Type 1) lie beneath the semilunar valves in the conal or outlet septum, non-committed VSDs (Type 2) are confluent with and involve the membranous septum and are bordered by an atrioventricular valve not in proximity of the great vessels, inlet VSDs (Type 3) involve the inlet of the right ventricular septum immediately inferior to the atrioventricular valve apparatus, and muscular VSDs (Type 4) are completely surrounded by muscle (Fig. 3).[18] Localizations were post-hoc compared with echocardiography and the surgical reports (Fig. 4). Sensitivity and specificity of CT for the detection of a VSD was calculated for all 154 patients using 2D echocardiography as reference.

2.7. Radiation dose

Radiation exposure was assessed as volumetric CT dose index (CTDIvol), referring to a 32 cm acrylic phantom, and dose length product (DLP). Effective dose (ED) was assumed as DLP*k, using an individual, linear interpolation of the conversion factors reported in literature[19] for chest CT at 80 kV between neonates (k_I = 0.0823 mSv/mGy*cm) and 1 year old children (k_{II} = 0.0525 mSv/mGy*cm) as a function of days of life (d) by the following equation:

$$ED = DLP * (k_{II} + \frac{d * (k_I - k_{II})}{365})$$

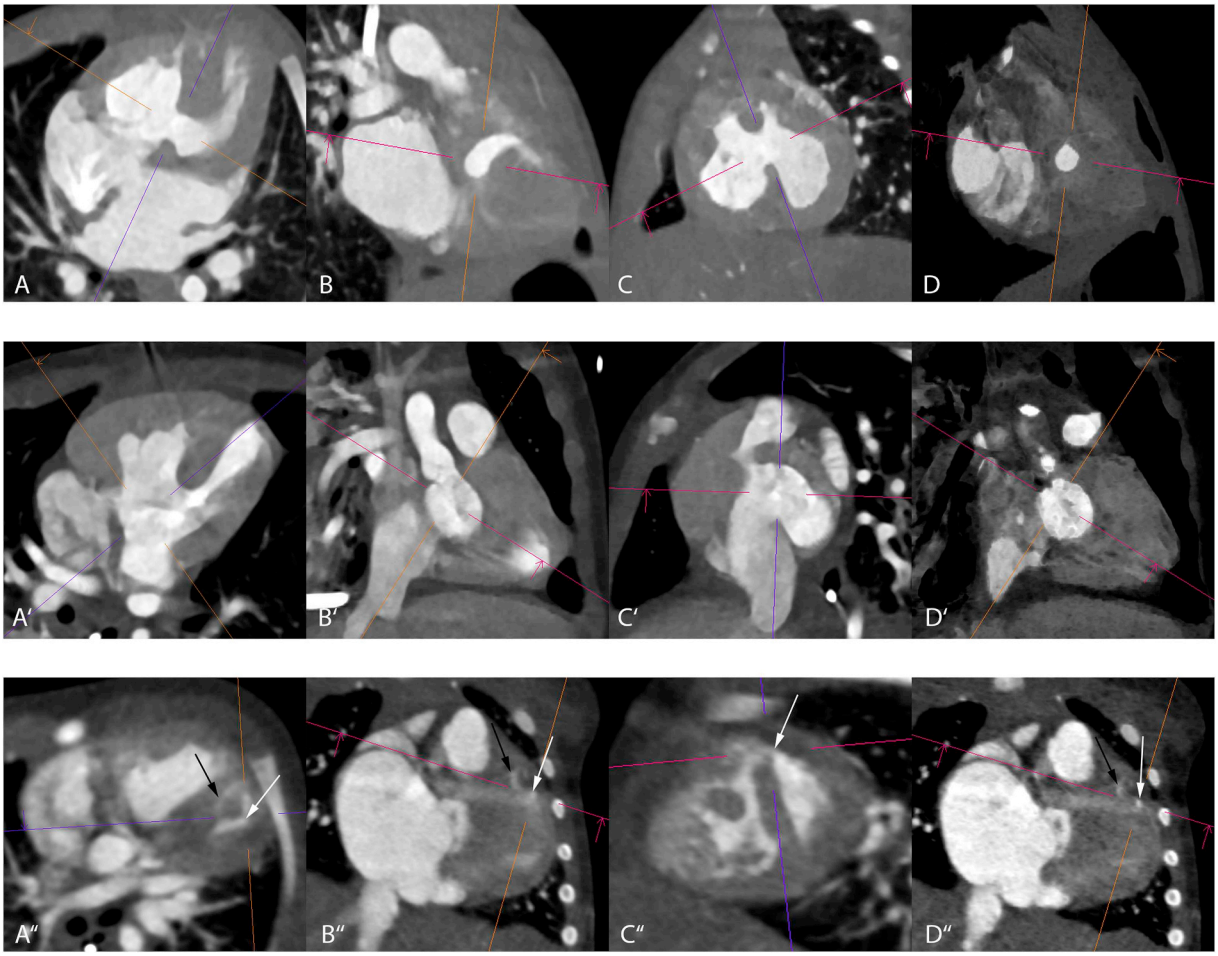

Fig. 3. Classification of ventricular septal defects: Adjusted four chamber (A-A''), two chamber (B-B'') and short axis (C-C'') MPR-planes of 1) a 17 days old boy with double outlet right ventricle and a non-committed type 2 VSD (A–D), 2) a 90 days old boy with an isolated inlet type 3 VSD (A′-D′) and 3) a 4 days old girl with hypoplastic left heart syndrome and small muscular type 4 defects (A''-D'', swiss cheese septum). Minimum intensity projections (MinIP) of the adjusted two chamber planes (D-D'') reduce partial volume effects and allow for a precise reproduction of the defects' anatomy. The comet tail appearance of the VSD in B can be identified as round shaped defect in D (slice thickness 8 mm), the thin atrial septum that contributes to the basal margin of the VSD in B′ is entirely reproduced in D' (slice thickness 11 mm) and the two tubular VSDs in B'' can be evaluated in their short axis by MinIP (slice thickness 5 mm) in D'' (black and white arrow).

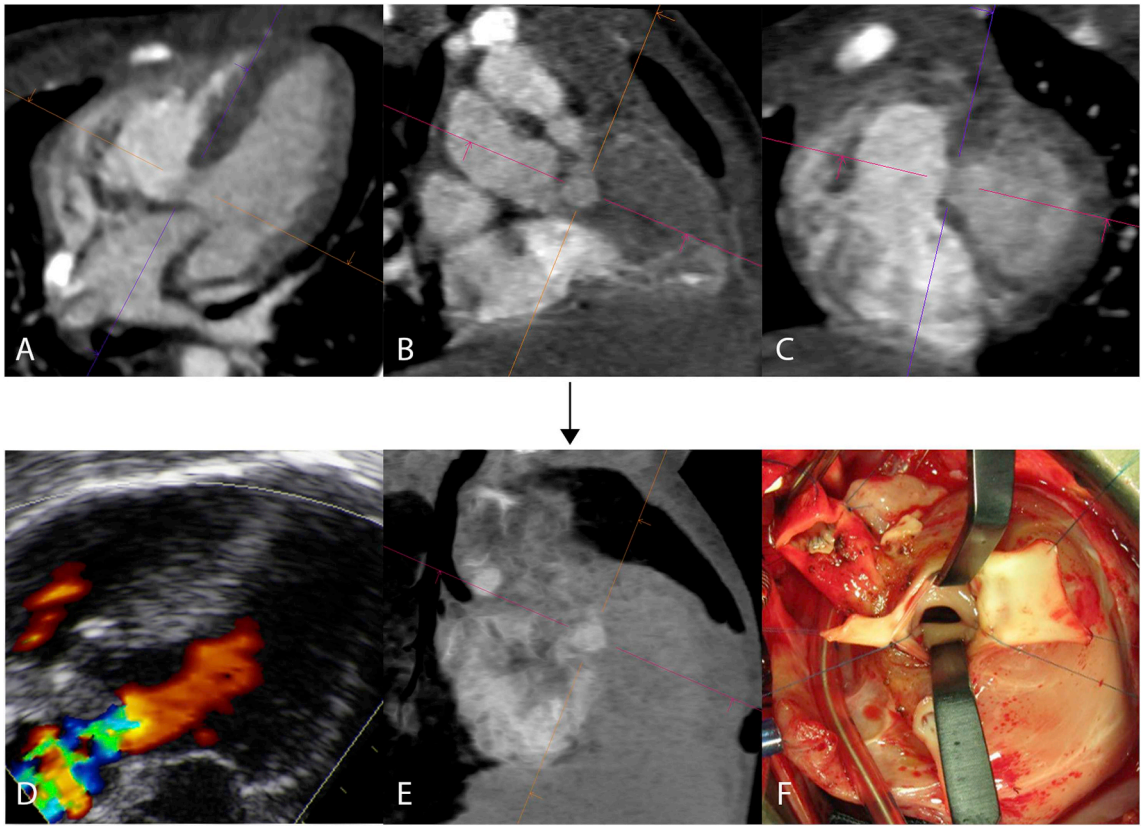

Fig. 4. Intraoperative correlation: Six days old boy with transposition of great arteries and a subaortic committed VSD (Type 1). The minimum intensity projection (E) with a slice thickness of 7.5 mm improves the reproduction of the margins of the VSD (6 mm) with good correlation to the surgical situs (8 mm, F). The measurements by echocardiography provided flow information while the measurement suffered from restricted angulations (3 mm, D).

2.8. Statistics

All statistical analyses were performed using the software package SPSS Statistics Version 21 (IBM, Somers, NY). Normal distribution of the data was tested by Kolmogorov-Smirnov tests. Normally distributed data is presented as mean ± standard deviation. Median and range are provided if no normal distribution was assumed. Interrater-correlation was calculated using the Spearman Rho test. Nonparametric Friedman ANOVA with post-hoc pairwise comparison was performed to evaluate the differences between the measurements obtained from surgery, echocardiography and CTA. Subtype analysis was carried out by Kruskal-Wallis ANOVA with pairwise post-hoc tests. Subgroup analysis of radiation dose was performed using Mann-Whitney-U test. The significance level was defined as $p < 0.05$.

3. Results

3.1. Patients

All patients were examined successfully without acute adverse effects. Intravenous sedation was needed for 8 from the 55 patients that were included in this study. Detailed patient information is shown in Table 2. The VSDs were associated with a non-communicating atrial septal defect (ASD) in 36 patients and were part of an atrioventricular septal defect (AVSD) in 5 patients. Other cardiac malformations were found in 41 patients and extra-cardiac malformations were associated in 49 patients, a combination of both was present in 35 patients (Table 3).

3.2. Surgery

The median time period between the preoperative CT examination and the surgical intervention was as low as 12 days, but ranged from 1 to 275 days. The median delay between echocardiography and surgery was 3 days (range 1–134 days). Surgical repair was part of a complex cardiac and extra-cardiac intervention in 34 patients, combined with only an additional extra-cardiac intervention in 7 patients, first step within the scope of a sequential approach in 7 patients and the only malformation requiring surgery in 7 patients. Transatrial surgical access was sufficient for the repair in 33 patients, ventriculotomy was required in 22 patients.

Table 2
Patient specifications, CT parameters and radiation dose.

	Median	Range
Age [days]	8	1–348
Size [cm]	52	38–72
Body weight [g]	3450	1650–8500
Scan length [cm]	17.4	14.3–22.4
Scan time [ms]	380	310–490
eff. mAs	70	38–236
CTDIvol [mGy]	0.36	0.15–2.07
DLP [mGy*cm]	6	2.3–38
Effective dose [mSv]	0.32	0.12–2.00
	Mean	**Standard deviation**
Body mass index [kg/m^2]	13.2	1.5
Body surface area [m^2]	0.24	0.06

Table 3
Associated cardiac and extra-cardiac malformations, combinations of the different pathologies were present within and between the subgroups.

Cardiac malformations	
Malposition of the great arteries	25
Common arterial trunk	6
Tetralogy of Fallot	6
Right ventricular outflow tract obstruction	12
Left ventricular outflow tract obstruction	6
Extracardiac malformations	
Pulmonary atresia or stenosis	9
Hypoplastic aorta	18
Right-sided aortic arch	8
Double aortic arch	1
Aortic isthmus stenosis	9
Coronary anomalies	10
Major aortopulmonary collateral arteries	7

3.3. CT technique

Body weight adapted contrast media injection (median 6 ml, range 4–20 ml) resulted in a median dose of 1.8 g iodine (range 1.2–6.0 g iodine). The mean heart rate was 138 ± 23 bpm during the examination. The automated heart phase selection algorithm resulted in an end-systolic mean cardiac phase of 44 ± 18% at the base of the heart and 54 ± 19% at the apex. Examinations from the third generation Dual-Source CT scanner had a significantly lower ED (0.22 mSv, range 0.12–0.73 mSv, n = 13) compared to the second generation (0.43 mSv, range 0.16–2.00 mSv, n = 42, p = 0.003). Cumulative exposure parameters are shown in Table 2.

3.4. Ventricular septal defects

Differences between the absolute sizes of the VSDs were statistically significant between echocardiography, CT and surgery ($p < 0.001$). The median intraoperative diameter size of the VSDs was 12.0 mm (range 3.0–25.0 mm, Fig. 5). Median CT-measurements of the longest absolute diameters were smaller without statistical significance in the post-hoc comparison (median 10.8 mm, range 2.8–18.1 mm, post-hoc $p = 0.09$). The median difference was 2.3 mm (range 0.0–13.5 mm), but the mean deviation was considerably smaller below a cut-off-value of 14 days delay to surgery (1.0 ± 2.6 mm) compared to above (3.2 ± 4.6 mm). Echocardiographic values were significantly smaller compared to both, intraoperative and measurements by CT (median 9.6 mm, range 3.0–18.5 mm, for both $p < 0.01$). The median difference compared to surgery was 3.2 mm (range 0.2–17.3 mm). Bland-Altman-Plots are shown in Fig. 6.

The median of the short axis obtained by CT was 7.3 mm (range 0.9–16.9 mm) and the median area was 0.63 cm^2 (0.05–2.15 cm^2). The interrater reliability for the longest and orthogonal shortest diameter was very good ($\varrho = 0.9$ and 0.8). The mean slice thickness used for the minimum intensity projection was 9.5 ± 2.5 mm.

Median normalized area was 2.4 cm^2/m^2 (range 0.3–10.0 cm^2/m^2) and median relative size was 0.52 (range 0.07–4.13). Size classifications following the absolute diameter were comparable between CT and the surgical measurements as shown in Table 4. However, 8 patients with non-restrictive defects were classified as restrictive by CT. Substantially more VSDs are considered non-restrictive if the normalized areas or the relative areas are used for the size classification (both $p < 0.01$).

The location of the VSD was classified as committed type 1 in the majority of patients (n = 44), followed by non-committed type 2 (n = 5), inlet type 3 (n = 5) and muscular type 4 (n = 1). Type 1 defects can be subdivided in subaortic-committed (n = 24), subpulmonary-committed (n = 12) or doubly committed (n = 8 including the 6 defects associated with a Truncus arteriosus communis). Only three type 1 VSDs and one type 2 VSD presented with an additional type 4 defect apical to the larger defect. The mean subtype size of the defects was 10.7 ± 2.6 mm for type 1, 11.9 ± 3.6 mm for type 2 and 13.5 ± 3.6 mm for type 3 without significant differences (all $p \geq 0.196$). Muscular type 4 defects were significantly smaller compared to the other types (4.4 ± 0.8 mm, $p < 0.001$). In only 2 patients (3.6%) the CT-classification of the location was different compared to the intraoperative finding. In both cases the underlying CHD was a malposition of the great arteries and both inconsistent classifications were retrospectively caused by misinterpretation of the arterial conus. Differences between VSD classification by echocardiography and surgery were found in 7 patients (12.7%). In 6 out of these cases type 2 or 3 defects were misinterpreted as type 1.

The sensitivity of CT for the detection of a VSD was 97.18% and the specificity 98.86%. Only two VSDs described by echocardiography could not be reproduced by CT (3 and 6 mm absolute diameter). On the other hand, also one defect that remained unnoticed by echocardiography was detected in the CTA.

4. Discussion

CTA provides a good 3D reproduction of CHD in general. We demonstrated that topographical evaluations of VSDs provide reliable results with a high sensitivity and specificity when MPR and MinIP techniques are used. Size measurements can be obtained with a high precision. Short diameter, normalized area and relative area can add valuable information that is only hardly obtained by two-dimensional echocardiography. Most of the VSDs had a relation to the arterial valves (80%, type 1), which was misinterpreted by echocardiography in 11% of all cases. Especially in cases of malpositioning, the arterial conus should be evaluated carefully. En-face views and virtual cardioscopic demonstrations additionally provide a three-dimensional understanding of the situs and help to evaluate surgical options. In comparison to the high periprocedural risk of the surgical repair the radiation exposure to the patients was reasonably low (0.32 mSv), and especially lower as previously described in literature for other techniques.[20] The low radiation dose and the possibility of free breathing, non-sedated cross-sectional imaging with short examination times and high spatial resolution can even favor CT over MRI in this collective.[21] However, the main advantage of this study is that the additional information about VSD anatomy can be used to enhance the multimodality approach for surgical workup of complex CHD.

The coexistence of CHD and VSDs is very high. Chelo et al. therefore concluded that a VSD should be evaluated by the examiner in case of CHD independent of the imaging method.[22] Due to its high availability and lack of radiation exposure two-dimensional echocardiography is the first imaging method of choice.[23] Complex CHD often require additional imaging due to the often spherical, distorted or irregular

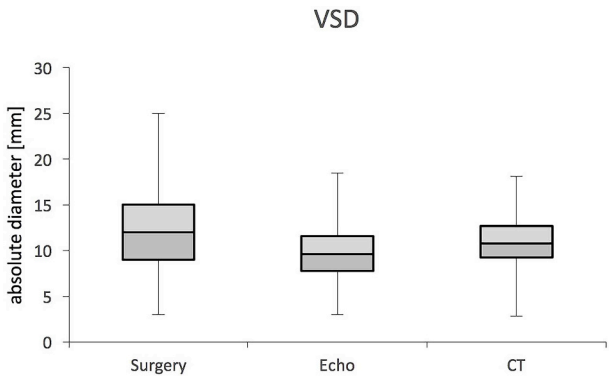

Fig. 5. Boxplot of absolute diameter of the ventricular septal defect (VSD) obtained from surgery, echocardiography and CT.

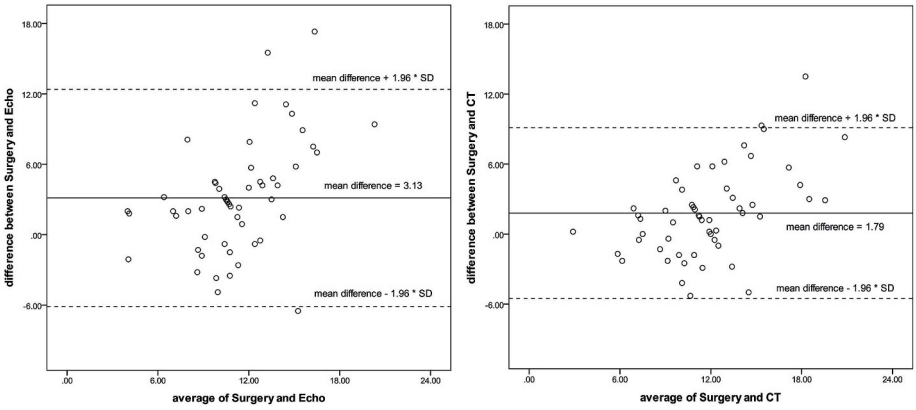

Fig. 6. Bland-Altman-Plot for surgery/echocardiography and surgery/CT.

Table 4
Size classification of the VSD from surgery and CT measurements.

	Diameter surgery	Diameter CT	Relative area CT	Normalized area CT
Small	19	21	7	1
Moderate	23	29	22	1
Large	13	5	20	53

margins of the VSDs that frequently do not fit into linear planes.[24] Especially in these patients CTA is able to simultaneously assess associated anomalies beyond the echocardiographic window with high spatial and temporal resolution and a low periprocedural risk.[25] Main type of associated malformations requiring such an elaborated imaging prior to surgery were malformations of the great arteries, outflow obstructions and coronary anomalies in our patient collective, which is in good agreement with the consensus recommendations about a multimodality imaging approach in the preoperative workup of CHD.[26,27] The good reproduction of VSDs in this study correlates well with the echocardiographic findings of Cheng et al., who reported better correlation to surgical findings using three-dimensional echocardiography compared to two-dimensional echocardiography.[5] The high interrater correlation (r = 0.8–0.9) underlines the robustness of the measurements and is comparable to the results of Chen et al. (r ~ 0.9) for three-dimensional echocardiography.[3] The large proportion of Type 1 defects in our collective is generally in good agreement with the literature.[28]

Some limitations need to be respected when interpreting the results of this retrospective study. First, the growth of the heart is very fast in young children and might also involve the VSDs. Hence the 19% inaccuracy of the CT measurements compared to the surgical measurements could be explained by the growing heart during the delay, which is supported by the substantially smaller differences for the subgroup below 14 days of delay (8%) compared to above (27%). Second, the intraoperative measurements are performed in cardioplegia. Thus, the comparison with the CT measurements might be biased by a non-physiologic relaxation and dilatation of the ventricles. Third, the CTA measurements are static and in most cases during end-systole. Hence, dynamic changes in size are not respected, while echocardiographic values were obtained in end-diastole in order to comply best with cardioplegia. Forth, CT is not able to provide dynamic flow information, which is easily assessed by MRI or echocardiography.[29] Fifth, although the radiation exposure is decreasing, concerns about stochastic damage cannot be waived in this especially sensitive collective.

5. Conclusion

In conclusion MinIP reconstructions of high pitch Dual-Source CT examinations allow for a precise reproduction of the location and size of VSDs in patients younger than one year. Additionally obtained values like short diameter, normalized area and relative areal can support the multimodality approach in this collective at a reasonably low radiation exposure. Therefore, whenever a CTA of patients with a CHD is performed, the presence of VSDs should be evaluated to provide information about size, orientation and localization for further clinical care, especially for patients with complex heart defects and anatomy.

Conflicts of interest

Speakers bureau: Lell, Uder, Wuest and May (Siemens Healthcare). Lell, Uder (Bayer Healthcare). Uder (Bracco, Medtronic).

Funding information

This research did not receive any specific grant from funding agencies in the public, commercial, or not-for-profit sectors.

Acknowledgments

We gratefully thank Petra Ruse for excellent patient examination, Julie-Marie Brügel for data assistance and Thomas Allmendinger for technological support.

David Nau: The present work was performed in partial fulfillment of the requirements for obtaining the degree “Dr med.”

Appendix A. Supplementary data

Supplementary data to this article can be found online at https://doi.org/10.1016/j.jcct.2019.01.023.

References

1. Rao PS. Consensus on timing of intervention for common congenital heart diseases: part I - acyanotic heart defects. *Indian J Pediatr.* 2013;80:32–38.
2. Satpathy MMB. *Clinical Diagnosis of Congenital Heart Disease.* Jaypee Brothers Medical Publishers; 2008:100–106.
3. Chen FL, Hsiung MC, Nanda N, Hsieh KS, Chou MC. Real time three-dimensional echocardiography in assessing ventricular septal defects: an echocardiographic-surgical correlative study. *Echocardiography.* 2006;23:562–568.
4. Sivakumar K, Anil SR, Rao SG, Shivaprakash K, Kumar RK. Closure of muscular ventricular septal defects guided by en face reconstruction and pictorial representation. *Ann Thorac Surg.* 2003;76:158–166.
5. Cheng TO, Xie MX, Wang XF, Wang Y, Lu Q. Real-time 3-dimensional echocardiography in assessing atrial and ventricular septal defects: an echocardiographic-surgical correlative study. *Am Heart J.* 2004;148:1091–1095.
6. Jenkins C, Monaghan M, Shirali G, Gurararaja R, Marwick TH. An intensive interactive course for 3D echocardiography: is 'crop till you drop' an effective learning strategy? *Eur J Echocardiogr.* 2008;9:373–380.
7. Seeger A, Krumm P, Hornung A, Schafer JF, Kramer U, Sieverding L. 3-D cardiac MRI in free-breathing newborns and infants: when is respiratory gating necessary? *Pediatr Radiol.* 2015;45:1448–1454.
8. Rompel O, Glockler M, Janka R, et al. Third-generation dual-source 70-kVp chest CT

angiography with advanced iterative reconstruction in young children: image quality and radiation dose reduction. *Pediatr Radiol.* 2016;46:462–472.
9. Ghoshhajra BB, Lee AM, Engel LC, et al. Radiation dose reduction in pediatric cardiac computed tomography: experience from a tertiary medical center. *Pediatr Cardiol.* 2014;35:171–179.
10. Ou P, Celermajer DS, Marini D, et al. Safety and accuracy of 64-slice computed tomography coronary angiography in children after the arterial switch operation for transposition of the great arteries. *J Am Coll Cardiol Img.* 2008;1:331–339.
11. Glockler M, Halbfass J, Koch A, et al. Preoperative assessment of the aortic arch in children younger than 1 year with congenital heart disease: utility of low-dose high-pitch dual-source computed tomography. A single-centre, retrospective analysis of 62 cases. *Eur J Cardiothorac Surg.* 2014;45:1060–1065.
12. Greil GF, Schoebinger M, Kuettner A, et al. Imaging of aortopulmonary collateral arteries with high-resolution multidetector CT. *Pediatr Radiol.* 2006;36:502–509.
13. Gerrah R, Bardo DM, Reed RD, Sunstrom RE, Langley SM. Adjustment of the surgical plan in repair of congenital heart disease: the power of cross-sectional imaging and three-dimensional visualization. *Congenit Heart Dis.* 2014;9(1):E31–E36.
14. Nakagawa M, Ozawa Y, Nomura N, et al. Utility of dual source CT with ECG-triggered high-pitch spiral acquisition (Flash Spiral Cardio mode) to evaluate morphological features of ventricles in children with complex congenital heart defects. *Jpn J Radiol.* 2016;34(4):284–291.
15. World Health Organization. *Global Database on Body Mass Index.* 2006; 2006http://www.euro.who.int/en/health-topics/disease-prevention/nutrition/a-healthy-lifestyle/body-mass-index-bmi, Accessed date: 29 August 2018.
16. Mosteller RD. Simplified calculation of body-surface area. *N Engl J Med.* 1987;317:1098.
17. Han BK, Rigsby CK, Hlavacek A, et al. Computed tomography imaging in patients with congenital heart disease Part I: rationale and utility. An expert consensus document of the society of cardiovascular computed tomography (SCCT). *J Cardiovasc Comput Tomogr.* 2015;9:475–492.
18. Jacobs JP, Burke RP, Quintessenza JA, Mavroudis C. Congenital heart surgery nomenclature and database project: ventricular septal defect. *Ann Thorac Surg.* 2000;69:S25–S35.
19. Deak PD, Smal Y, Kalender WA. Multisection CT protocols: sex- and age-specific conversion factors used to determine effective dose from dose-length product. *Radiology.* 2010;257:158–166.
20. Johnson JN, Hornik CP, Li JS, et al. Cumulative radiation exposure and cancer risk estimation in children with heart disease. *Circulation.* 2014;130:161–167.
21. Han BK, Overman DM, Grant K, et al. Non-sedated, free breathing cardiac CT for evaluation of complex congenital heart disease in neonates. *J Cardiovasc Comput Tomogr.* 2013;7(6):354–360.
22. Chelo D, Nguefack F, Menanga AP, et al. Spectrum of heart diseases in children: an echocardiographic study of 1,666 subjects in a pediatric hospital, Yaounde, Cameroon. *Cardiovasc Diagn Ther.* 2016;6:10–19.
23. Pettersen MD, Du W, Skeens ME, Humes RA. Regression equations for calculation of z scores of cardiac structures in a large cohort of healthy infants, children, and adolescents: an echocardiographic study. *J Am Soc Echocardiogr.* 2008;21:922–934.
24. Kilner PJ, Geva T, Kaemmerer H, Trindade PT, Schwitter J, Webb GD. Recommendations for cardiovascular magnetic resonance in adults with congenital heart disease from the respective working groups of the European society of cardiology. *Eur Heart J.* 2010;31:794–805.
25. Hausmann P, Stenger A, Dittrich S, et al. Application of dual-source-computed tomography in pediatric cardiology in children within the first year of life. *Fortschr Röntgenstr.* 2016;188:179–187.
26. Han BK, Rigsby CK, Leipsic J, et al. Computed tomography imaging in patients with congenital heart disease, Part 2: technical recommendations. An expert consensus document of the society of cardiovascular computed tomography (SCCT): endorsed by the society of pediatric radiology (SPR) and the north American society of cardiac imaging (NASCI). *J Cardiovasc Comput Tomogr.* 2015;9(6):493–513.
27. Prakash A, Powell AJ, Geva T. Multimodality noninvasive imaging for assessment of congenital heart disease. *Circ Cardiovascular imaging.* 2010;3(1):112–125.
28. Rojas CA, Jaimes C, Abbara S. Ventricular septal defects: embryology and imaging findings. *J Thorac Imag.* 2013;28:W28–W34.
29. Mahmood M, Haque SS, Siddique MA, Ahmed CM, Hossain Z. Doppler evaluation of left to right shunt (Qp/Qs) in patients with isolated ventricular septal defect (Vsd). *Mymensingh Med J.* 2007;16:181–186.